

CO ($a^3\Pi$) quenching at a metal surface: Evidence of an electron transfer mediated mechanism

Fabian Grätz,^{1,2,3} Daniel P. Engelhart,^{1,2} Roman J. V. Wagner,^{1,2} Gerard Meijer,^{3,a)}
 Alec M. Wodtke,^{1,2} and Tim Schäfer^{1,2,b)}

¹Max-Planck-Institut Für Biophysikalische Chemie, Karl Friedrich-Bonhoeffer-Institut, Am Fassberg 11,
 37077 Göttingen, Germany

²Georg-August-Universität Göttingen, Institut für Physikalische Chemie, Tammannstr. 6,
 37077 Göttingen, Germany

³Fritz-Haber-Institut der Max-Planck-Gesellschaft, Abteilung Molekülphysik, Faradayweg 4-6,
 14195 Berlin, Germany

(Received 30 April 2014; accepted 20 June 2014; published online 29 July 2014)

We observe a strong influence of molecular vibration and surface temperature on electron emission promoted by the de-excitation of metastable CO($a^3\Pi$) on a clean Au(111) surface using a molecular beam surface scattering apparatus. The de-excitation is independent of incidence translational energy. These observations appear incompatible with existing theories of metastable particle de-excitation on metal surfaces, which are based on the Auger effect. Instead, they strongly suggest a mechanism involving formation of a transient anion whose lifetime is similar to the vibrational period of the CO molecule. © 2014 AIP Publishing LLC. [<http://dx.doi.org/10.1063/1.4887777>]

INTRODUCTION

Understanding the decay pathways of excitation in surface adsorbates is a fundamental aspect of surface physics and chemistry and the wide variety of solid properties makes this an open field of study where much remains to be discovered. Insulators offer phonon baths that may soak up excitation by mechanical interactions.¹ Metals possess both phonons and electrons that can accept adsorbate excitation – and due to failure of the Born-Oppenheimer approximation, nuclear and electronic motion can be strongly coupled.^{2,3} For interactions of ground electronic state molecules with metal surfaces, energy exchange between molecular vibration and the metal's electron-hole pairs has been well documented.^{3–16} When vibrational excitation exceeds the solid's work function, electron emission is observed,^{16–19} sometimes even with high yield.¹⁵ It is also now well established that electron transfer mediates the energy exchange between molecular vibration and electrons in the metal.

Elucidating energy transfer of electronically excited molecules at metals remains challenging, despite its obvious relevance to important topics like surface photochemistry and photophysics.^{20–24} One reason for this is that lifetimes of electronically excited adsorbates tend to be extremely short^{25,26} – 10–100 fs – reflecting the strong coupling of the molecule's and the metal's electronic motion. Such short lifetimes present technical challenges to performing experiments.

An alternative approach avoiding the problems of short lifetimes employs scattering beams of electronically excited

molecules from surfaces, an approach that is particularly useful for metastable states.^{27–29} There are surprisingly few examples of this type of experiment to be found in the literature. Some of this work was motivated by a desire for detectors for metastable species^{29–31} – metastable quenching can result in electron emission, which is easily detectable with electron multipliers. In these examples, ultra-high vacuum (UHV) methods were not always used, meaning the properties of the surface were not always well-defined. On the other hand, atomically clean crystalline insulator surfaces have been used for dynamics experiments with metastable CO($a^3\Pi$)^{27,28} – from now on referred to as CO*. This work revealed inefficient quenching of the excited electronic state. Only recently have the first experiments of this type been carried out for metastable collisions on single crystal metals, prepared under UHV conditions.³²

While experiments with molecules are rare, metastable atoms and atomic ions have been commonly used in UHV surface-science studies. Here, collisional quenching at a metal surface often results in electron emission. The resulting electron energy distributions are sensitive to surface electronic structure and especially to adsorbates. These phenomena serve as the basis of a now well-established surface analytical tool: metastable quenching spectroscopy (MQS).^{33–35}

As a result of this method's utility, a great deal of effort has gone into understanding the mechanism of electron emission³⁶ and we now know that the Auger effect³⁷ plays an important role. For example, when metastable He atoms with $1s2s$ orbital occupation collide at a metal surface, an electron from the conduction band of the metal may relax to fill the $1s$ orbital, simultaneously ejecting the $2s$ electron – this is called Auger de-excitation (AD). Alternatively, the $2s$ electron may be transferred to the metal entering unoccupied orbitals above the Fermi level – called resonant ionization (RI) – and subsequently, two electrons of the conduction band may engage in

^{a)}Current address: Radboud University Nijmegen, Institute for Molecules and Materials, Heijendaalseweg 135, 6525 AJ Nijmegen, The Netherlands

^{b)}Author to whom correspondence should be addressed. Electronic mail: tschae4@gwdg.de.

an Auger neutralization (AN) process, one electron ending up in the $1s$ orbital of the He and the other being excited and often ejected to the vacuum.

For molecular metastable collisions at surfaces, new quenching mechanisms become possible. In particular, nearly all molecules can bind an electron forming a negative ion, something that the noble gas atoms of MQS cannot. Hence, electron transfer from the solid to the incoming molecular metastable may be an important step in the quenching event. Indeed, several authors have suggested that metastable molecules can quench by means of resonant charge transfer (RCT) from the surface, in which a temporary molecular anion is formed.^{23,24,38–40} Electron transfer is also known to play a central role in mediating energy exchange between molecular vibration and electrons in the metal.^{3,13–16}

In a recent publication, we reported observations on the quenching of CO^* at a clean Au(111) surface, which appeared incompatible with an AD mechanism.³² The electron emission yield was high ($\gamma = 13\%$), surprisingly large for such a low energy metastable if AD were the mechanism. In addition, we found unexpected *enhancement wings* in the signals that arose from optically pumped vibrationally excited CO^* . We pointed out that the vibrational enhancement of electron emission is incompatible with an extended AD mechanism.³¹

In this paper, we extend our study of CO^* quenching at Au(111), systematically employing Franck-Condon pumping (FCP) under conditions where ionization/depletion is unimportant. This allows us to quantify the effect of vibration on electron emission. We also characterize the surface temperature and translational energy dependence of electron emission. These observations provide strong evidence of the importance of transient negative ion formation in the quenching at metal surfaces of electronically excited molecules.

EXPERIMENTAL

All measurements were performed in a new apparatus, designed to study quantum-state specific interactions of molecules with well-defined surfaces at controlled translational incidence energies. It combines a pulsed molecular beam, laser excitation, and a Stark decelerator^{41,42} with a differentially pumped UHV scattering chamber equipped with surface preparation and characterization instruments (Figure 1). A 360 m/s supersonic beam of carbon monoxide is created via expansion of 20% CO in Xe in a pulsed valve (*General Valve* series 99) cooled to 260 K. After skimming the beam, a narrow bandwidth laser system⁴³ is used to pump CO to the first electronically excited state via the $a^3\Pi_1(v=0, J=1) \leftarrow X^1\Sigma^+(v=0, J=1)$ transition at 206 nm. Molecules in this long-lived state – the lifetime is 2.63 ms⁴⁴ – may be readily manipulated by electric fields due to the large dipole moment of 1.37 D. Prior to entering the decelerator, the CO^* is deflected by 3.5° in a pulsed electrostatic hexapole lens and passes through a differential pumping aperture, thereby removing the carrier gas and electronic ground state CO from the molecular beam. The translational energy of CO^* can be tuned within the range of 0.36 meV–38 meV (50–512 m/s) using a 131 stage Stark decelerator.

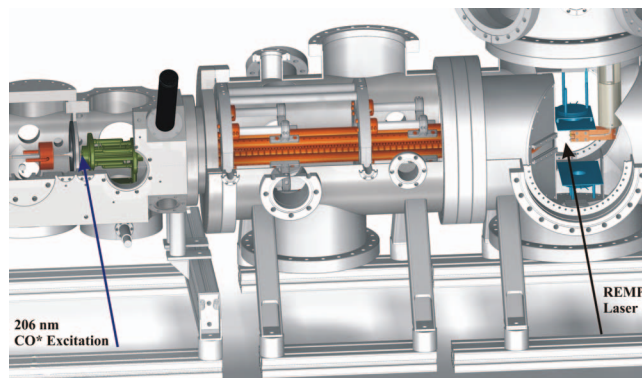


FIG. 1. Cutaway drawing of the apparatus. 20% CO in Xe expands through a pulsed valve (red). The molecular beam is skimmed 3-cm down-stream and optically excited to the $a^3\Pi_1$ state with a narrow bandwidth OPO laser system operating at 206 nm. Deflecting the CO^* molecules by 3.5° with an electrostatic hexapole focuser (green) then creates a molecular beam of pure CO^* . After passing the decelerator (orange), CO^* molecules enter the UHV chamber where they scatter from a Au(111) surface, mounted to a movable sample holder (salmon). REMPI and FCP laser beams can be directed in front of the surface. Two MCP assemblies (blue) are mounted above (electron detection) and below (REMPI ion detection) the molecular beam axis.

The temperature-controlled gold surface is mounted 62 mm behind the exit of the decelerator in differentially pumped scattering chamber, maintained at a pressure of $\sim 2 \times 10^{-10}$ mbar. We clean the Au(111) surface by Ne^+ sputtering and subsequent annealing to 900 K prior to experiments, and confirm its purity by Auger electron spectroscopy (*STAI*B ESA-100). CO^* molecules can be detected prior to surface collision by 1+1 resonance enhanced multiphoton ionization (REMPI) using a pulsed laser (*Spectra Physics* PDL-2) resonant with the $b^3\Sigma^+ \leftarrow a^3\Pi$ transition 21 mm upstream from the surface. An electric field of 140 V/cm extracts CO^+ ions produced by REMPI and electrons emitted upon collision of CO^* with the gold surface towards two separate MCP detectors. The overlap of the molecular beam with the laser is optimized by mounting a $200 \mu\text{m}$ wide slit behind the decelerator parallel to the direction of the laser beam.

We employed FCP to create controlled vibrational state distributions of CO^* at a velocity of 360 m/s. See Figure 2. CO ($a^3\Pi, v=0$) is pumped to the $b^3\Sigma^+(v=0 \text{ or } 1)$ state by a pulsed laser beam (*Continuum* Sunlite Ex OPO) that crosses the molecular beam 19 mm upstream from the surface. The lifetimes of the $b^3\Sigma^+(v=0 \text{ and } 1)$ states are less than 70 ns⁴⁵ – this ensures that all $b^3\Sigma^+$ molecules fluoresce to the $a^3\Pi$ state before they hit the surface, producing CO^* vibrational distributions governed by Franck-Condon factors. The FCP laser intensity is kept weak enough to avoid depletion of the CO^* beam by ionization but strong enough to saturate the $b^3\Sigma^+ \leftarrow a^3\Pi$ transition.

Electron emission signals were recorded as the surface temperature was varied between 50 and 900 K. For each surface temperature, we obtain a reference time-of-flight trace of the molecular beam pulse by scanning the delay time between excitation and REMPI lasers. Comparison with the time-of-flight profile obtained from electrons emitted from the surface allows us to normalize the electron emission to the incoming, available metastable molecules. In a similar fashion, we

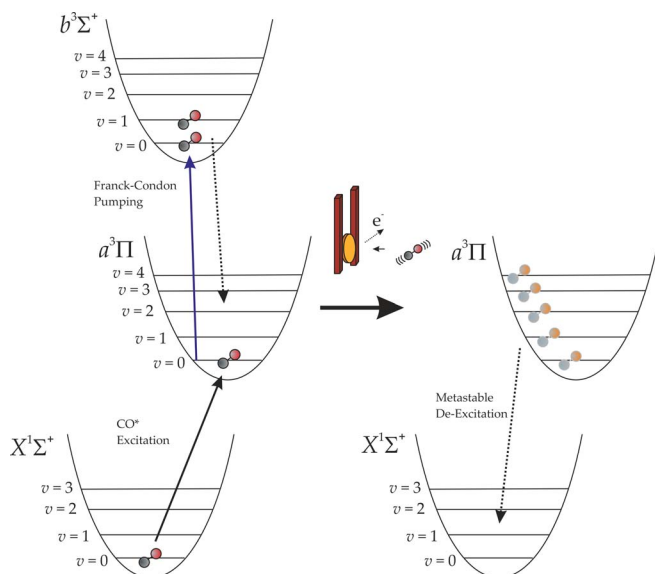


FIG. 2. Concept of preparing vibrationally excited CO^* by Franck-Condon pumping. After deceleration of the $\text{CO}^*(v=0)$ molecules, this state is pumped to $b^3\Sigma^+(v=0 \text{ or } 1)$. Spontaneous emission populates $\text{CO}^*(v > 0)$ according to known Franck-Condon factors.

determine γ as a function of incident CO^* velocity. In all measurements, we considered the finite lifetime of the $a^3\Pi$ state and corrected the signals accordingly.

RESULTS

Figure 3 shows the vibrational enhancement of electron emission resulting from CO^* quenching at a Au(111) surface. Here, the lower panel shows the electron emission signal as the FCP laser wavelength is scanned. The enhancement appears at wavelengths coincident with known transitions⁴⁶ in the $b^3\Sigma^+(v) \leftarrow a^3\Pi(v=0)$ absorption system ($b^3\Sigma^+(v=1)$ – dark red and $b^3\Sigma^+(v=0)$ – light blue). These transitions coincide with those of the 1+1 REMPI spectra shown in the upper panel.

For a quantitative analysis of the vibrational enhancement, the excitation efficiency of the FCP process has to be taken into account. The weaker of the two observed peaks in the spectrum of Figure 3 is due to the single $R_{32}(1)$ transition, while the stronger peak contains the two non-resolved $P_{32}(1)$ and $R_{12}(1)$ transitions. Assuming saturation, only 2/3 of all molecules will be excited to the $b^3\Sigma^+$ state at the center of the stronger peak. Scaling the signal accordingly,⁴⁷ we obtain an enhancement of electron emission by a factor of $\varepsilon = 1.47$ and $\varepsilon = 1.51$ when pumping is performed via the $b^3\Sigma^+(v=0)$ and the $b^3\Sigma^+(v=1)$ state, respectively.

The observed enhancement factors reflect an average over the different vibrational state distributions in the $a^3\Pi$ state shown in the inset of Figure 3. It is possible to single out groups of levels which contribute more strongly or weakly to the overall signal. Notably, pumping either via $b^3\Sigma^+(v=0)$ or $b^3\Sigma^+(v=1)$ lead to a comparable enhancement of electron emission, despite the fact that the population in $a^3\Pi(v=1-3)$ is much smaller and the population in $a^3\Pi(v=0)$ is much larger in the latter case. Thus, the con-

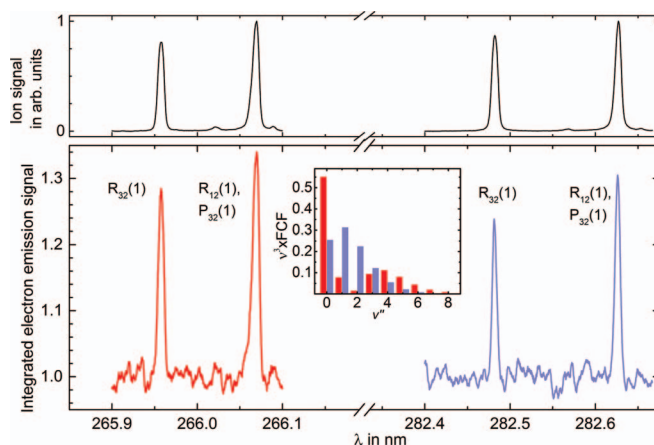


FIG. 3. Lower panel: Electron emission vs. FCP laser wavelength. Transitions to $b^3\Sigma^+(v=1)$ (left, dark red) and $b^3\Sigma^+(v=0)$ (right, light blue) enhance the emission. Upper panel: simultaneously recorded REMPI ion signal. Inset: the CO^* vibrational population distributions arising from FCP; they are computed from the known Franck-Condon factors.⁴⁶ The electron emission signal is scaled to the previously determined maximum enhancement of 1.31 of the stronger peak when pumping via the $b^3\Sigma^+(v=0)$ state.³² The spectrum is recorded under conditions such that the $b^3\Sigma^+ \leftarrow a^3\Pi$ transition is saturated. Note that because the two peaks in the spectrum consist of a different number of ro-vibrational transitions, the laser excitation efficiency is 1/2 (2/3) for the smaller (bigger) of the two peaks. When scaling the two peaks accordingly, the resulting actual enhancement is the same within the experimental uncertainty. See text and Ref. 47 for details. Data on the right side are reproduced from our previous paper.³²

tribution to electron emission from states with $a^3\Pi(v \geq 4)$, must be much larger than for $a^3\Pi(v=1-3)$. One can calculate the enhancement relative to the $a^3\Pi(v=0)$ state for the two groups of vibrational levels by solving a system of two coupled linear equations using basic linear algebra. In this way, we obtain averaged electron emission yields, γ_v , for vibrational levels, v , of the $a^3\Pi$ state of $\gamma_{1-3} = (1.49 \pm 0.14)\gamma_0$ and $\gamma_{\geq 4} = (2.62 \pm 0.39)\gamma_0$. While our experiment does not yield state-specific results, the analysis clearly demonstrates a strong enhancement of electron emission with increasing vibrational quantum number.

The effect of surface temperature on electron emission resulting from $\text{CO}^*(v=0)$ quenching at Au(111) is shown in Figure 4. While γ remains nearly constant between 50 K and 250 K, we observe an unexpectedly strong increase in electron emission above this temperature – $(27 \pm 7)\%$ more electrons are released at $T_s = 900$ K than at $T_s = 250$ K. To our knowledge, this is the first report of a strong influence of surface temperature on metastable quenching at a clean metal surface.^{36,48}

We also studied the incidence translational energy dependence of γ , shown in Figure 5. Within the measurement uncertainty, electron emission is independent of incidence translational energy over the range studied.

DISCUSSION

In this work, we introduce CO^* with orbital configuration $1\sigma^2 1\sigma^{*2} 2\sigma^2 2\sigma^{*2} 1\pi^4 3\sigma^2 1\pi^{*1}$ to a metal surface. The system relaxes to the molecular ground state $1\sigma^2 1\sigma^{*2} 2\sigma^2 2\sigma^{*2} 1\pi^4 3\sigma^2$ with emission of an electron. We

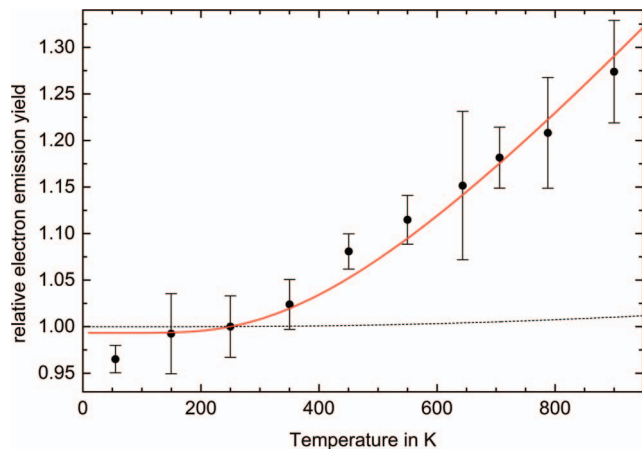


FIG. 4. Temperature dependence of electron emission yield. Experimental data points are scaled to 250 K. If we integrate a temperature dependent Fermi Function from 80 meV below the Fermi level to infinite energy, the solid red line results. This is strong evidence that only electrons initially very close to the Fermi level lead to electron emission. The Zubek model³¹ (dashed black line) fails to reproduce the data.

discuss this in terms of two possible mechanisms: AD and RCT. As mentioned above, AD has been commonly invoked to explain de-excitation of atomic metastables in collisions at metals. For CO*, AD occurs when an electron from the metal's conduction-band relaxes filling the 3σ orbital, simultaneously ejecting the $1\pi^*$ electron. See Figure 6. The $1\pi^*$ electron is ejected by its repulsive interaction with the relaxing conduction-band electron;³⁷ hence, the molecule must typically be in close proximity to the solid so the electrons are not shielded from one another.^{35,36} Furthermore, no transient anion is formed. In RCT, an electron first tunnels from the surface, forming CO⁻ with orbital occupation $1\sigma^2 1\sigma^* 2\sigma^2 2\sigma^* 1\pi^4 3\sigma^2 1\pi^* 1$ – the π^* electron is subsequently ionized on a time-scale similar to that of molecular vibration. The finite lifetime of the anion is a consequence of the electron's binding energy to CO being dependent on C–O inter-nuclear separation as well as its distance from the surface.

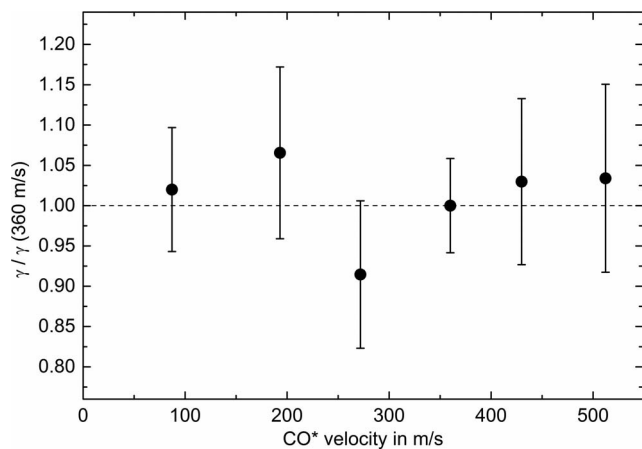


FIG. 5. Variation of γ with normal velocity of CO*, relative to γ (360 m/s). Within the uncertainty of the experiment, no effect is observed, as indicated by the dashed line. We also show statistical errors calculated as standard deviation of multiple measurements.

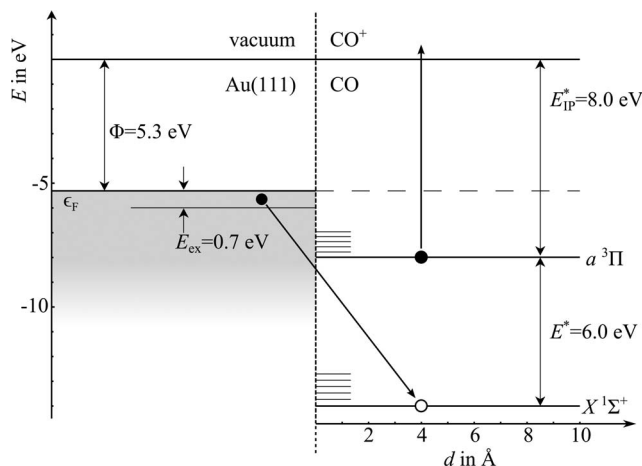


FIG. 6. Energy diagram of metastable CO* quenched at a Au(111) surface by an Auger de-excitation mechanism. An electron from the metal's conduction band fills the 3σ orbital, simultaneously ejecting the $1\pi^*$ electron. See text. If the conduction band electron is not within 0.7 eV of the Fermi level, electron escape to the vacuum fails.

AD has been invoked to explain relaxation of molecular metastables in collisions at metals; however, it appears to be incompatible with the observations of this work. First of all, the absolute electron yield of CO* on Au³² is comparable to the AN yield of He⁺ on Tungsten.³⁶ This is surprising since AD scales strongly with the ionization energy of the particle, which is four times larger for He⁺ compared to CO*. Second, AD is sudden – hence, molecular vibrational transitions must reflect Franck-Condon factors. Zubek³¹ suggested the electron emission yield is proportional to the excess energy beyond the work function, $E_{\text{ex}} = E^* - \Phi$, summed over all possible Franck-Condon weighted molecular decay channels.^{30,32} This model predicts $\gamma_{1-3}/\gamma_0 = 1.02$ and $\gamma_{\geq 4}/\gamma_0 = 1.10$, significantly underestimating the experimentally observed vibrational enhancement. Furthermore, the electron emission from AD can occur for electrons up to 0.7 eV below the Fermi level (Figure 6); hence, a strong surface temperature dependence for electron emission cannot be easily explained – the predictions on surface temperature dependence of Zubek's³¹ model are shown as a dashed line in Figure 4. See the Appendix for details.

In contrast to AD, RCT can explain the key experimental observations – the strong surface temperature dependence, the vibrational enhancement, the large electron yield, and the independence from translational energy.

In Figure 4, the solid red line shows the energy integral of the temperature dependent Fermi Function, where the lower limit to integration is 80 meV below the Fermi level and the upper limit is unbounded. The excellent agreement with the experimental surface temperature dependence strongly suggests that electrons close to the Fermi level – within 80 meV – dominate the de-excitation process. This is hard to rationalize by an AD mechanism but entirely reasonable for RCT – to see this we must consider the energetics of CO⁻ formation when CO* collides with a Au surface.

The ground state of CO⁻ has been extensively studied both theoretically^{49,50} and with electron scattering.^{51,52} It possesses $^2\Pi$ symmetry and lies 1.7 eV above the ground state of

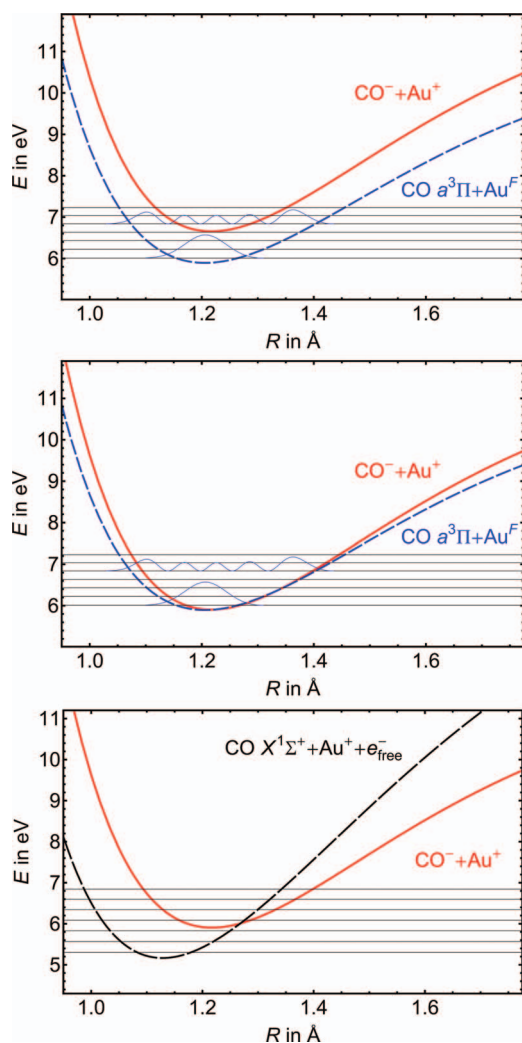


FIG. 7. (Upper panel) Potential energy curves for the CO-Au(111) system as a function of C–O internuclear distance at asymptotic surface distances. The dashed blue curve represents vibration of the CO* with an electron at the Fermi level. Vibrational energy levels of CO* are depicted by horizontal lines. The solid red curve represents vibration of the CO⁻ after electron transfer from the solid has occurred. Thus, an electron transfer from Au to CO is represented by a transition from the dashed blue to the solid red curve. At this surface distance electron transfer is energetically forbidden. (Middle panel) Same as in upper panel but for an image charge stabilization of the anion state of 0.75 eV, corresponding to a surface distance of 5.4 Å. An electron transfer can now happen for electrons at the Fermi level if the C–O distance is greater than 1.2 Å. (Lower panel) Same as middle panel. Instead of the CO* potential energy curve, the dashed black curve now shows the CO ground state with an electron at the vacuum level, i.e., the potential energy curve is shifted 5.3 eV upward in energy. Horizontal lines depict the vibrational energy levels of ground state CO.

CO. When the CO molecule is separated far from the gold surface, transferring an electron from gold to CO requires 7.0 eV – recall that the work function of Au is 5.3 eV. The CO* excitation energy is only 6.0 eV – hence, there is insufficient energy to form the anion. See Figure 7 (upper panel), which shows potential energy curves obtained from the literature mentioned above. As the anion approaches the metal surface it is increasingly stabilized due to image charge interaction.^{53,54} At ~ 5.4 Å, a distance where electron transfer is expected to be efficient,^{11,18} CO⁻ is isoenergetic with CO*, if the CO bond is stretched. See Figure 7 (middle panel).

Hence, electron transfer first becomes possible for a stretched CO molecule, where tunneling may occur for electrons in the energetically topmost part of the conduction band, whose population is most sensitive to surface temperature. The fact that only the top 80 meV of the band participate suggests that the electron transfer happens for distances between ~ 5.4 Å and 5.0 Å.

The vibrational enhancement can also be understood within this RCT model. Figure 7 (lower panel) shows the stability of the anion with respect to the neutral CO ground-state as a function of CO bond length, also at a molecule metal distance of 5.4 Å. Note that the dashed black curve is shifted by 5.3 eV because the electron originally at the Fermi level is now at the vacuum level. Here, we see that only at extended CO bond lengths is the anion more stable than the CO ground state. Hence, if an electron is transferred to the CO* near the outer turning point of vibration as suggested by Figure 7 (middle panel), the electron will be ejected near the inner turning point, and the lifetime of the anion is likely to be on the order of half a vibrational period, $\sim 10^{-14}$ s. As the vibrational quantum number increases, the lifetime of the resonance does too, since the molecule spends a longer time at extended CO bond lengths. The resulting narrower resonance width also interacts more selectively with electrons near the Fermi level. Hence, the probability of the initial charge transfer step is higher for vibrationally excited molecules.

We also point out that the large yield observed in this work is consistent with those seen in vibrationally promoted electron emission,¹⁵ a similar mechanism involving electron transfer.

To summarize, the CO* must reach a distance of about 5.0–5.4 Å from the surface at which point electron transfer is possible but only for electrons within 80 meV of the Fermi level. The electron transfer is more efficient if the CO bond is stretched beyond its equilibrium distance, such that the electron is captured near the outer turning point of vibration. Within about 10 fs, the CO bond has compressed and the electron is released. The short lifetime of the anion prevents the translational energy from having an influence, since on this short time-scale, motion toward the surface is negligible.

While the RCT model provides a qualitative explanation of our observations of CO* de-excitation on Au(111), it cannot yet be considered fully proven – further study is needed. Experiments where CO* impinges on a surface with rare gases layers of varying thickness directly probe the surface distance dependence of electron emission – RCT occurs at larger surface distances than AD.^{35,36} Electron transfer has recently been shown to exhibit a strong orientation dependence¹⁴ – experiments with oriented CO* are also attractive. Measurements of CO final vibrational state distributions as well as emitted electron energy distributions would also shed more light on this problem.

SUMMARY AND CONCLUSION

We have studied the influence of molecular vibration, surface temperature, and incidence translational energy on the electron emission efficiency in the de-excitation of CO in its $a^3\Pi$ state on Au(111). The electron emission yield, γ_v ,

for individual groups of vibrational levels is $\gamma_{1-3} = (1.48 \pm 0.14)\gamma_0$ and $\gamma_{\geq 4} = (2.59 \pm 0.38)\gamma_0$. In addition, we have observed a strong influence of surface temperature, which leads to a rise in γ of $(27 \pm 7)\%$ between 250 K and 900 K. Varying the incidence velocity of the CO* beam shows no observable influence on γ . These experimental findings can be explained by a resonant charge transfer de-excitation mechanism that proceeds via the anionic $^2\Pi$ shape resonance, whereas they appear incompatible with an Auger de-excitation mechanism.

ACKNOWLEDGMENTS

We acknowledge support from Deutsche Forschungsgemeinschaft (DFG) and the National Science Foundation (NSF) under Grant No. CHE0724038. A.M.W. also thanks the Alexander von Humboldt Foundation for support under a Humboldt Professorship. R.J.V.W. gratefully acknowledges a Ph.D. fellowship granted by the Fonds der Chemischen Industrie.

APPENDIX: METASTABLE DE-EXCITATION IN THE AD MODEL

In this appendix, we briefly discuss the extension of the Auger de-excitation model to take into account the vibration of a molecule quenching at a metal surface following the model of Zubek.³¹

The emitted electron in the AD model stems from an Auger process, which happens instantly on the timescale of molecular vibration. Therefore, the molecules will relax to a vibrational distribution in the electronic ground state governed by Franck-Condon overlap. The electron emission yield, $\gamma_{v'}$, for an initial vibrational level v' can be approximated by

$$\gamma_{v'} \propto \sum_{v''} q(v'', v') \times \int_{\epsilon_F - E_{\text{ex}}(v'', v')}^{\infty} f(\epsilon, T) \mathcal{D}(\epsilon) d\epsilon. \quad (\text{A1})$$

Here, $f(\epsilon, T)$ is the Fermi function, $q(v'', v')$ is the Franck-Condon factor between the ground state vibrational level, v'' , and the metastable state vibrational level, v' , and ϵ_F is the Fermi energy. $E_{\text{ex}}(v'', v') = E^*(v'', v') - \Phi$ is the excess energy for electron emission, where $\Phi = 5.31$ eV is the work function of Au(111) and $E^*(v'', v')$ is the energy difference between the levels v'' and v' . The electronic density of states in the conduction band, $\mathcal{D}(\epsilon)$, can be taken as a constant in the relevant energy range.⁵⁵ The approximation introduced by Borst³⁰ and Zubek³¹ is obtained for constant $\mathcal{D}(\epsilon)$ and by setting $f(\epsilon, T) = f(\epsilon, 0\text{K})$. In this model, averaged electron emission yields of $\gamma_{1-3} = 1.02\gamma_0$ and $\gamma_{\geq 4} = 1.10\gamma_0$ are predicted. The simple model for the AD mechanism thus predicts an electron emission enhancement of 2% and 10%, which underestimates our observed enhancement by one order of magnitude.

To explain how a T_S dependence might arise in the AD mechanism, consider Auger de-excitation is exoenergetic by 0.7 eV at asymptotic separation assuming that the vibrational quantum number is conserved in the interaction. More

precisely, direct Auger de-excitation only results in electron emission if the energy of the conduction band electron relative to the Fermi energy, $\epsilon_F - \epsilon$, meets the condition $E_{\text{ex}}(v'', v') - (\epsilon_F - \epsilon) > 0$. At any non-zero T_S , relaxation is possible forming vibrationally excited states for which the excess energy is not sufficient to eject an electron at $T_S = 0$ K. Using Eq. (A1), the influence of T_S on electron emission can be calculated (dotted curve of Fig. 4). This clearly does not explain the observed effect. The data can only be understood with this model if we assume that at least 84% of CO($a^3\Pi$) relaxes to vibrational levels of CO($X^1\Sigma^+$) with $v'' \geq 3$. This, however, violates the Franck-Condon principle on which this model is based.

¹G. E. Ewing, *Acc. Chem. Res.* **25**, 292 (1992).

²E. Hasselbrink, *Curr. Opin. Solid State Mater. Sci.* **10**, 192 (2006).

³A. M. Wodtke, D. Matsiev, and D. J. Auerbach, *Prog. Surf. Sci.* **83**, 167 (2008).

⁴Y. Huang, A. M. Wodtke, H. Hou, C. T. Rettner, and D. J. Auerbach, *Phys. Rev. Lett.* **84**, 2985 (2000).

⁵T. Schäfer, N. Bartels, K. Golibrzuch, C. Bartels, H. Kockert, D. J. Auerbach, T. N. Kitsopoulos, and A. M. Wodtke, *Phys. Chem. Chem. Phys.* **15**, 1863 (2013).

⁶A. M. Wodtke, J. C. Tully, and D. J. Auerbach, *Int. Rev. Phys. Chem.* **23**, 513 (2004).

⁷C. Bartels, R. Cooper, D. J. Auerbach, and A. M. Wodtke, *Chem. Sci.* **2**, 1647 (2011).

⁸K. Golibrzuch, A. Kandratsenka, I. Rahinov, R. Cooper, D. J. Auerbach, A. M. Wodtke, and C. Bartels, *J. Phys. Chem. A* **117**, 7091 (2013).

⁹I. Rahinov, R. Cooper, D. Matsiev, C. Bartels, D. J. Auerbach, and A. M. Wodtke, *Phys. Chem. Chem. Phys.* **13**, 12680 (2011).

¹⁰Q. Ran, D. Matsiev, D. J. Auerbach, and A. M. Wodtke, *Phys. Rev. Lett.* **98**, 237601 (2007).

¹¹J. D. White, J. Chen, D. Matsiev, D. J. Auerbach, and A. M. Wodtke, *J. Chem. Phys.* **124**, 064702 (2006).

¹²N. Shenvi, S. Roy, and J. C. Tully, *Science* **326**, 829 (2009).

¹³R. Cooper *et al.*, *Angew. Chem., Int. Ed.* **51**, 4954 (2012).

¹⁴N. Bartels, K. Golibrzuch, C. Bartels, L. Chen, D. J. Auerbach, A. M. Wodtke, and T. Schäfer, *Proc. Natl. Acad. Sci. U.S.A.* **110**, 17738 (2013).

¹⁵N. H. Nahler, J. D. White, J. LaRue, D. J. Auerbach, and A. M. Wodtke, *Science* **321**, 1191 (2008).

¹⁶J. D. White, J. Chen, D. Matsiev, D. J. Auerbach, and A. M. Wodtke, *Nature (London)* **433**, 503 (2005).

¹⁷J. LaRue, T. Schäfer, D. Matsiev, L. Velarde, N. H. Nahler, D. J. Auerbach, and A. M. Wodtke, *Phys. Chem. Chem. Phys.* **13**, 97 (2011).

¹⁸J. L. LaRue, T. Schäfer, D. Matsiev, L. Velarde, N. H. Nahler, D. J. Auerbach, and A. M. Wodtke, *J. Phys. Chem. A* **115**, 14306 (2011).

¹⁹N. H. Nahler and A. M. Wodtke, *Mol. Phys.* **106**, 2227 (2008).

²⁰M. Drabbels, C. G. Morgan, and A. M. Wodtke, *J. Chem. Phys.* **103**, 7700 (1995).

²¹M. Grätzel, *Nature (London)* **414**, 338 (2001).

²²M. J. Comstock *et al.*, *Phys. Rev. Lett.* **99**, 038301 (2007).

²³N. Lorente, D. Teillet-Billy, and J. P. Gauyacq, *Surf. Sci.* **432**, 155 (1999).

²⁴P. Stracke, F. Wieggershaus, S. Krischok, and V. Kemper, *Surf. Sci.* **396**, 212 (1998).

²⁵H. Petek, H. Nagano, M. J. Weida, and S. Ogawa, *J. Phys. Chem. B* **105**, 6767 (2001).

²⁶D. Velic, A. Hotzel, M. Wolf, and G. Ertl, *J. Chem. Phys.* **109**, 9155 (1998).

²⁷R. T. Jongma, G. Berden, T. Rasing, H. Zacharias, and G. Meijer, *Chem. Phys. Lett.* **273**, 147 (1997).

²⁸R. T. Jongma, G. Berden, T. Rasing, H. Zacharias, and G. Meijer, *J. Chem. Phys.* **107**, 252 (1997).

²⁹S. J. Humphrey, C. G. Morgan, A. M. Wodtke, K. L. Cunningham, S. Drucker, and R. W. Field, *J. Chem. Phys.* **107**, 49 (1997).

³⁰W. L. Borst, *Rev. Sci. Instrum.* **42**, 1543 (1971).

³¹M. Zubek, *Chem. Phys. Lett.* **149**, 24 (1988).

³²F. Grätz, D. P. Engelhart, R. J. V. Wagner, H. Haak, G. Meijer, A. M. Wodtke, and T. Schäfer, *Phys. Chem. Chem. Phys.* **15**, 14951 (2013).

³³H. Conrad, G. Ertl, J. Küppers, S. W. Wang, K. Gérard, and H. Haberland, *Phys. Rev. Lett.* **42**, 1082 (1979).

- ³⁴F. Bozso, J. Arias, J. T. Yates, R. M. Martin, and H. Metiu, *Chem. Phys. Lett.* **94**, 243 (1983).
- ³⁵Y. Harada, S. Masuda, and H. Ozaki, *Chem. Rev.* **97**, 1897 (1997).
- ³⁶H. D. Hagstrum, *Phys. Rev.* **96**, 336 (1954).
- ³⁷E. H. S. Burhop, *Proc. R. Soc. London, Ser. A* **148**, 272 (1935).
- ³⁸H. Müller, D. Gador, and V. Kempter, *Surf. Sci.* **338**, 313 (1995).
- ³⁹H. Müller, R. Hausmann, H. Brenten, and V. Kempter, *Chem. Phys.* **179**, 191 (1994).
- ⁴⁰J. Marbach, F. X. Bronold, and H. Fehske, *Eur. Phys. J. D* **66**, 106 (2012).
- ⁴¹H. L. Bethlem, G. Berden, and G. Meijer, *Phys. Rev. Lett.* **83**, 1558 (1999).
- ⁴²S. Y. T. van de Meerakker, H. L. Bethlem, N. Vanhaecke, and G. Meijer, *Chem. Rev.* **112**, 4828 (2012).
- ⁴³L. Velarde, D. P. Engelhart, D. Matsiev, J. LaRue, D. J. Auerbach, and A. M. Wodtke, *Rev. Sci. Instrum.* **81**, 063106 (2010).
- ⁴⁴J. J. Gilijamse, S. Hoekstra, S. A. Meek, M. Metsaelae, S. Y. T. v. de Meerakker, G. Meijer, and G. C. Groenenboom, *J. Chem. Phys.* **127**, 221102 (2007).
- ⁴⁵A. J. Smith, R. E. Imhof, and F. H. Read, *J. Phys. B* **6**, 1333 (1973).
- ⁴⁶C. V. V. Prasad, G. L. Bhale, and S. P. Reddy, *J. Mol. Spectrosc.* **121**, 261 (1987).
- ⁴⁷The correct scaling is obtained in the following way: The enhancement, ε , for a given population of CO* molecules produced via Franck-Condon pumping is defined by $\gamma = \varepsilon\gamma_0$. One third of all CO* molecules in the FCP laser volume are not laser-excited, thus their enhancement is unity. The measured enhancement, ε_m , is thus related to the actual enhancement caused by laser-excited molecules, ε , by the relation $1/3 + 2/3 \times \varepsilon = \varepsilon_m \Rightarrow \varepsilon = 3/2 \times \varepsilon_m - 1/2$.
- ⁴⁸H. Hotop, in *Experimental Methods in the Physical Sciences*, Part B, edited by F. B. Dunning and G. H. Randall (Academic Press, 1996), Vol. 29, p. 191.
- ⁴⁹V. Laporta, C. M. Cassidy, J. Tennyson, and R. Celiberto, *Plasma Sources Sci. Technol.* **21**, 045005 (2012).
- ⁵⁰L. A. Morgan and J. Tennyson, *J. Phys. B* **26**, 2429 (1993).
- ⁵¹J. Zobel, U. Mayer, K. Jung, and H. Ehrhardt, *J. Phys. B* **29**, 813 (1996).
- ⁵²M. Allan, *Phys. Rev. A* **81**, 042706 (2010).
- ⁵³The image charge stabilization, E_{img} , has been calculated according to $E_{\text{img}}(d) = -\frac{3.6}{d-s} \text{ eV } \text{ \AA}$, where d is the surface distance in \AA , and the parameter s is assumed to be 0.6.
- ⁵⁴J. A. Appelbaum and D. R. Hamann, *Phys. Rev. B* **6**, 1122 (1972).
- ⁵⁵P. H. Citrin, G. K. Wertheim, and Y. Baer, *Phys. Rev. Lett.* **41**, 1425 (1978).